Environ. Sci. Technol. **2002**, *36,* 403−410

Carbon Tetrachloride Transformation in a Model Iron-Reducing Culture: Relative Kinetics of Biotic and Abiotic Reactions

MICHAEL L. MCCORMICK,[†] EDWARD J. BOUWER,[‡] AND PETER ADRIAENS*,[†]

Department of Civil and Environmental Engineering, University of Michigan, Ann Arbor, Michigan 48109-2125, and Department of Geography and Environmental Engineering, Johns Hopkins University, Baltimore, Maryland 21218

Contributions of biotic (cell-mediated) and abiotic (mineral-mediated) reactions to carbon tetrachloride (CT) transformation were studied in a model iron-reducing system that used hydrous ferric oxide (HFO) as the electron acceptor, acetate as the substrate, and *Geobacter metallireducens* as a representative dissimilative iron-reducing bacteria (DIRB). Over a period of 2−3 weeks, nanoscale magnetite particles, Fe_3O_4, were consistently formed as a product of iron respiration in this system. CT transformation rates were measured independently in resting cell suspensions of *G. metallireducens* or in suspensions of washed magnetite particles recovered from spent cultures. Protein and surface area-normalized expressions were derived for the biotic and abiotic reaction rates, respectively. Using the yield of total protein and magnetite surface area formed during growth in the model system as a basis for comparison, the mineral-mediated (abiotic) reaction was estimated to be 60−260-fold faster than the biotic reaction throughout the incubation period. We conclude that *G. metallireducens* induces CT transformation in this system primarily through the formation of reactive mineral surfaces rather than via co-metabolic mechanisms. The findings indicate that reactive biogenic minerals could play a significant role in the natural attenuation of chlorinated solvents in iron-reducing environments. A novel approach for stimulating reductive transformation of contaminants may be to enhance the formation of reactive biogenic minerals in situ.

Introduction

The prevalence of aquifers contaminated with chlorinated solvents has sparked great interest in developing bioremediation schemes to degrade these pollutants in situ. Carbon tetrachloride (CT) is one of the most frequently encountered chlorinated solvent contaminants in groundwaters of the United States (*1*). Although relatively stable, and therefore persistent in the environment, CT has been shown susceptible to degradation in anaerobic environments by both biotic (*2*, *3*) and abiotic mechanisms (*4*−*7*). Much of the research on the microbial transformation of CT has focused on the roles of methanogenic, sulfate-reducing, and nitrate-reducing bacteria (*2*, *3*, *8*−*10*). In addition, a number of bacteria have been isolated that directly couple respiration to reductive dechlorination (halorespiration) (*11*−*13*). Another significant physiological class of microorganisms, the dissimilative iron-reducing bacteria (DIRB), couple the oxidation of organic substrates to ferric iron (Fe^{III}) reduction to obtain energy (iron respiration). Because Fe^{III} is the predominant electron acceptor in many aquifer and lake sediments (*14*−*16*) and because DIRB appear ubiquitous in the subsurface (*17*), interest has grown in the potential contributions of these bacteria to the transformation of chlorinated solvents in anaerobic environments.

The half-reaction reduction potential ($E^{\circ\prime}$) for the hydrogenolysis of CT under environmentally relevant conditions is relatively high (+673 mV), reflecting the fully oxidized state of carbon and chlorine's high electronegativity (Figure 1). By comparison, the reduction potentials of common electron carriers found in anaerobic bacteria are significantly lower (see Figure 1), indicating that these compounds are thermodynamically feasible reductants of CT. Such reactions depend on low specificity in the biological reductants and are termed "co-metabolic" to reflect their fortuitous nature. Biochemical mechanisms are not, however, the only means to degrade CT in iron-reducing sediments. As a consequence of iron respiration, DIRB produce copious amounts of ferrous iron (Fe^{II}) that can accumulate in solution, adsorb to the surfaces of surrounding minerals, or become incorporated into new "biogenic" minerals. The half-reaction reduction potentials associated with these ferrous iron species also fall well below that required for CT reduction (Figure 1) (*20*).

It has long been recognized that both cell-mediated (biotic) and mineral-mediated (abiotic) reactions may contribute to the reductive transformation of contaminants in iron-reducing environments (*21*−*23*). Yet attempts to quantify the relative contributions of biotic and abiotic reactions in these complex systems are rare. To date, the only strictly biological studies of CT transformation by a DIRB are those of Picardal et al. (*24*, *25*) and Petrovskis et al. (*26*), both of which employed strains of the highly versatile facultative anaerobe *Shewanella putrefaciens*. Although the phylogeny of iron respiration appears broadly distributed among prokaryotes (*17*), no other DIRB has yet been reported to transform CT. Several studies have demonstrated that Fe^{II} adsorbed to ferric oxides and hydroxides can abiotically reduce CT whether the source of the Fe^{II} is microbial reduction (*27*−*30*), chemical reduction (*29*), or direct addition (*27*, *28*). Working with *S. putrefaciens*, Kim and Picardal (*29*) and Picardal et al. (*30*) demonstrated that CT transformation rates increased as much as 10-fold in the presence of ferric hydroxide solids and correlated this to the formation of biogenic Fe^{II} adsorbed to mineral surfaces. Abiotic reduction of CT has also been demonstrated with a variety of Fe^{II}-containing minerals (*4*−*6*, *31*−*35*). The mixed valence iron oxide magnetite ($Fe^{II}Fe^{III}{}_2O_3 = Fe_3O_4$), a common product of microbial iron reduction, has been shown to reduce CT (*34*, *35*), nitroaromatics (*36*−*38*), and Cr(VI) (*39*).

The goals of this study were to (i) determine if the DIRB, *G. metallireducens*, was capable of directly transforming CT, (ii) characterize the kinetics of CT transformation by biogenic magnetite produced by *G. metallireducens*, and (iii) evaluate the relative contributions of cell-mediated (biotic) versus mineral-mediated (abiotic) reactions to the overall transformation of CT in a model iron-reducing system that used

* Corresponding author phone: (734)763-8032; fax: (734)763-2275; e-mail: adriaens@engin.umich.edu.
[†] University of Michigan.
[‡] Johns Hopkins University.

10.1021/es010923+ CCC: $22.00
Published on Web 01/04/2002

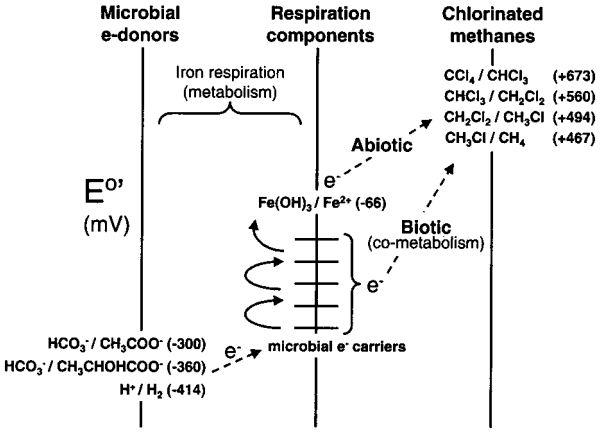

FIGURE 1. Thermodynamic consideration of the biotic and abiotic pathways for electron transfer from common microbial electron donors to chlorinated methanes in an iron-reducing environment. Half-reaction reduction potentials calculated assuming environmental conditions (pH 7.0, $[Cl^-] = [HCO_3^-] = [acetate] = [lactate] = 10^{-3}$ M, $[Fe^{2+}] = 10^{-5}$ M). Some example electron carriers found in anaerobic bacteria include ferredoxin ox/red (−390 mV), NAD^+/NADH (−320 mV), cyt-c_3 ox/red (−290 mV), FAD/FADH (−220 mV), and menaquinone ox/red (−75 mV) from Madigan et al. (*18*). Redox potentials for chlorinated methanes taken from Totten and Roberts (*19*).

G. metallireducens and in which magnetite was the primary mineral product of iron respiration.

Experimental Section

Cell Culturing and Mineral Biogenesis. All operations requiring strictly anaerobic conditions were performed in an anaerobic glovebag filled with 98% N_2 and 2% H_2 (Coy Laboratory Products, Ann Arbor, MI). Purified water was prepared using a Milli-Q plus water system (Millipore Corp., Bedford, MA). All chemicals were of ACS or reagent grade. *G. metallireducens* was maintained in defined iron-reducing media (IR media) composed of 100 mM hydrous ferric oxide (HFO)(s), 10 mM acetate, and trace nutrients in a bicarbonate buffer (2.5 g L^{-1} $NaHCO_3$, 20% CO_2/80% N_2 headspace, initial pH 7.0) (*40*). Fresh media was purged for 30 min with N_2(g) and then boiled under vacuum at room temperature to establish anoxic conditions. For resting cell studies, *G. metallireducens* was grown in 2-L batches of 50 mM Fe^{III}−citrate media amended with 10 mM acetate and buffered at pH 7.0 with 25 mM 3-(*N*-morpholino)-2-hydroxypropanesulfonic acid (MOPSO), modified from ref *41*. Cells were harvested at the late exponential phase of growth (Fe^{II} > 45 mM) by centrifugation (8000*g*, 10 min, 4 °C), washed twice, then resuspended in anoxic buffer (pH 7.0, 10 mM MOPSO), and distributed to reaction vials. Unless stated otherwise, all incubations and kinetic studies were conducted at 30 °C.

Biogenic magnetite (Fe_3O_4) was produced in IR media containing ~200 mM HFO and 20 mM acetate. Formation of a black magnetic phase was usually evident within 10−20 days after inoculation with *G. metallireducens*. The solids were collected magnetically and then washed in fresh anoxic buffer (pH 7.0, 10 mM MOPSO) with mild sonication to dislodge cells and cell debris. After four sonication/washes, the solids were distributed into reaction vials as a slurry. Three sonication/washes were found sufficient to reduce the protein content (i.e., biomass) of the solids to below detection by the protein assay employed (see below).

The bulk proportion of Fe^{II}/Fe^{TOT} in the biogenic magnetite was determined by complete digestion of the solids in anoxic 5 N HCl followed by partial neutralization (equal-volume addition of 4.5 M NaOH) and then determination of Fe^{II} by the Ferrozine assay (*42*) and of total iron (Fe^{TOT}) by atomic absorption spectroscopy. Fe^{III} was determined by difference. Specimens for transmission electron microscopy (TEM) were collected by dipping holey carbon Cu grids into anoxic aqueous suspensions of the biogenic particles and allowing the grids to dry in the anaerobic glovebag. Samples were examined at normal and high resolution on a JEOL JEM-4000EX high-resolution transmission electron microscope. Micro-probe crystallographic data were collected using selected area electron diffraction (SAED). X-ray diffraction (XRD) analyses were conducted using a Rigaku Rotaflex rotating anode XRD apparatus (Cu Kα radiation, 40 kV, 100 mA). Freshly collected "wet" XRD samples were mounted on glass slides in the anaerobic glovebag and then sealed under tape to prevent sample oxidation during analysis. "Dry" XRD samples were prepared by freeze-drying and back-filling under N_2(g) to prevent potential oxidation. The dried solids appeared to be stable in the atmosphere (no visible color change) and were analyzed without protective tape. Specific surface area (SSA) measurements were made using a Micromeritics ASAP 2010 surface area analyzer (Micromeritics Corp., Norcross, GA) applying the method of Brunauer, Emmett, and Teller (BET) with N_2 as the adsorbate gas.

Biomass Measurements. Subsamples of the resting cell suspensions were collected and frozen (−20 °C) at the beginning of each biological experiment. Later, cells were thawed and disrupted by alkaline lysis (pH adjusted to 10.5−11.5 with 1 N NaOH, held 10 min at 70 °C plus 30 s immersion in a low-energy sonication bath). After centrifugation, the supernatant was recovered and analyzed for total protein using the Bradford assay (Bio-Rad Inc.) and bovine serum albumin (BSA) standards. To correlate protein measurements to cell density, total protein determinations for freshly harvested and washed *G. metallireducens* cells (Fe^{III}−citrate grown) were compared with direct cell counts using a Petroff-Hausser bacteria counting chamber and phase contrast microscopy.

Samples for protein analysis that contained cells and iron oxide solids were subjected to the same alkaline lysis protocol described above. After centrifugation, the supernatant was decanted, neutralized, freeze-dried, and then resuspended in 25 mM MOPSO (pH 7.0) containing 2% sodium dodecyl sulfate (SDS). The resulting suspension was concentrated by membrane filtration (3 kDa cutoff) (Microcon YM-3, Millipore Corp., Bedford, MA). The protein concentrate was washed with 500 μL of Milli-Q water to reduce the SDS concentration then recovered from the membranes using five sequential 100-μL Milli-Q water rinses. As SDS is known to interfere with the Bradford assay, the solution was analyzed for total protein using the Micro-BCA assay (Pierce Chemical Co.). BCA measurements of protein in *G. metallireducens* extracts were, on average, 27% higher than Bradford assay results and were adjusted down proportionally to make protein measurements comparable.

Transformation Rate Studies. CT transformation rates were evaluated in batch reactions using either resting cell suspensions of *G. metallireducens* or biogenic magnetite particles produced by this same strain. Reactions were conducted in glass serum vials containing a nitrogen headspace (headspace volume = 53.3−55.6% of the vial volume) and sealed with gastight Teflon-coated gray butyl rubber septa. Vials were spiked with an anoxic saturated aqueous solution of CT, inverted, and incubated in the dark at 30 °C in a reciprocating water bath (300 rpm). Nonreactive controls containing only buffer and CT were run in parallel. CT and volatile products were quantified over time by headspace sampling and direct injection gas chromatography on a Hewlett-Packard 6890 series GC system fitted with a HP-5 column (30 m × 0.32 mm × 0.25 μm) operated isothermally (30 °C) using flame ionization detection (FID). External standards were prepared from methanol stocks in gastight

serum vials with the same gas to liquid volume ratio as the reaction vials. At least 30 min was allowed after spiking with CT to permit headspace equilibration before collecting the first sample. The initial CT concentrations (CT_0) were estimated by extrapolating the fitted decay curves to $t = 0$ h. All reported rate constants were adjusted to account for the effect of headspace partitioning on the reaction kinetics using the method described by Butler and Hayes (*43*). Values for the dimensionless Henry's law constant for CT (mol L^{-1}_{gas}/mol L^{-1}_{liquid}) were calculated after Gossett (*44*) (at 30 °C, the value of 1.54 was applied).

To examine strictly biotic CT transformation rates, vials were prepared in duplicate with resting cell suspensions of *G. metallireducens* at 325, 163, 65, and 33 ± 2 mg of protein L^{-1}. The vials were amended with 10 mM acetate to ensure that cells were not reductant-limited prior to CT addition ($CT_0 \approx 4.0$ μM). The effect of initial CT concentration on biotic transformation rates was examined using a constant biomass of 294 ± 22 mg of protein L^{-1} and CT_0 ranging from 2 to 40 μM. To determine if Fe^{II} adsorption on cells affected transformation rates, ferrous chloride ($FeCl_2$) was added to resting cell suspensions (pH 7.0, 20 mM MOPSO) to achieve initial concentrations of approximately 100, 300, and 600 μM Fe^{II}(aq). After 1 h of mixing, a subsample of each suspension was collected and analyzed for total ferrous iron. A second aliquot of the suspension was centrifuged to remove cells and sampled again. Cell associated Fe^{II} was calculated by difference. Vials were then sealed, spiked ($CT_0 \approx 7.5$ μM), and monitored for transformation.

To obtain strictly abiotic CT transformation rates, vials were prepared in duplicate with biogenic magnetite at mass loadings of approximately 8, 14, 18, or 24 g L^{-1}. Magnetite was used from cultures of different ages (124 and 565 days) to see if mineral reactivity changed with time. The magnetite particles were washed and resuspended under similar solution conditions to the cell studies (pH 7.0, 10 mM MOPSO) with the addition of 100 mM $NaClO_4$ for ionic strength adjustment and 0.5 mM $FeCl_2$ to inhibit desorption of surface Fe^{II}. Despite the addition of $FeCl_2$, a slow increase in aqueous ferrous iron was observed in both suspensions. After 7 days, the percent change in concentration was less than 1% per day. The vials were then spiked ($CT_0 \approx 19$ μM) and monitored for transformation in identical manner to the biological kinetic studies.

Transformation Rate Studies in Whole Culture. The combined contributions of biotic and abiotic reactions to CT transformation were assessed in a whole culture of *G. metallireducens* growing in IR media (~160 mM HFO, 20 mM acetate) during the early, middle, and late stages of iron reduction. At multiple time points, 5.0-mL samples of the whole culture (cells plus iron oxides) were collected and transferred as a slurry to gastight serum vials (11.25 mL) under anaerobic conditions, spiked with CT ($CT_0 \approx 13-15$ μM), and monitored for transformation rates as described above. Parallel 5.0-mL subsamples of the culture slurry were analyzed for total mineral surface area or total protein as described above.

Results and Discussion

Product Formation. Chloroform (CF) was the only identified dechlorination product in the *G. metallireducens* suspensions, accounting for 15−30% of the consumed CT. In the abiotic experiments, the CF yield varied from 35 to 45%. Dichloromethane or chloromethane were not observed in either the biotic or the abiotic systems. The transformation of CT via biotic and abiotic pathways in identical systems to those used in this study resulted in the formation of CF, CH_4, cell-bound products, and other unidentified products as discussed elsewhere (*35*).

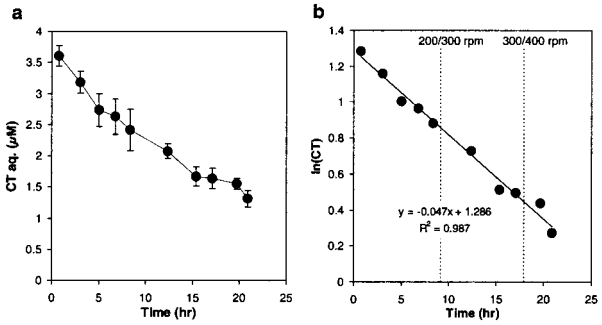

FIGURE 2. (a) CT depletion in resting cell suspension of *G. metallireducens* (biomass = 325 ± 2 mg of protein L^{-1}, $CT_0 = 3.7$ μM). (b) Natural-log transformed concentration data. Time points at which the mixing rate for the vials was increased from 200 to 300 rpm and then from 300 to 400 rpm are indicated. Data points report the average of duplicate vials. Error bars represent one standard deviation.

Biotic Transformation of CT by *G. metallireducens*. The transformation of CT by resting cells of *G. metallireducens* (325 ± 2 mg of protein L^{-1}) is shown in Figure 2a. The linearity of the log-transformed concentration data (Figure 2b) suggests that first-order transformation kinetics adequately describe the rate data (eq 1). The invariance of the pseudo-first-order decay rate while mixing rates increased from 200 to 400 rpm indicates that gas−liquid mass transfer was not rate limiting in this system (Figure 2b).

$$-\frac{dC}{dt} = k_{obs}C \quad (1)$$

No CT transformation was observed in vials containing only buffer or autoclaved cells. At reaction times longer than 25 h, biotic rates diminished, suggesting loss of cell activity either by toxicity or starvation (data not shown). For this reason, the rate analyses for all biotic experiments were limited to time periods of approximately 25 h or less. Pseudo-first-order rate constants were determined at each biomass loading by nonlinear least-squares fitting of the time course data to eq 1 (SAS/STAT Version 6, SAS Institute Inc., Cary, NC). After accounting for headspace partitioning, the pseudo-first-order rate constants were found to be linearly dependent on *G. metallireducens* biomass, allowing a biomass-normalized rate constant to be estimated, $k'_{biotic} = 3.90 \times 10^{-4} \pm 2.9 \times 10^{-5}$ h^{-1} (mg of protein)$^{-1}$ L (Figure 3).

If the biotic reaction truly obeys first-order kinetics with respect to CT, then the rate coefficient should remain constant regardless of the starting CT concentration. The effect of initial CT concentration on the protein-normalized pseudo-first-order rate constants is shown in Figure 4. Although the plot appears to approach a constant value at high concentrations, it is clearly not first-order at low concentrations (<15 μM). The observed trend in reaction rates can be explained by invoking a two-site Michaelis−Menten model of the following form:

$$-\frac{dC}{dt} = \left(\frac{\nu_1^{max}}{K_1 + C}\right)X_0C + \left(\frac{\nu_2^{max}}{K_2}\right)X_0C \quad (2)$$

where C is the aqueous CT concentration (μM), X_0 is the biomass concentration (mg of protein L^{-1}), ν^{max} is the maximum specific rate constant for the first (ν_1^{max}) or second (ν_2^{max}) reaction site (μM h^{-1} (mg of protein)$^{-1}$ L), and K is the affinity for CT at the first (K_1) or second (K_2) reaction site (μM). The model assumes that the first site has a moderately high affinity for CT ($C \geq K_1$) and that the second site has a low affinity ($C \ll K_2$), thus C is dropped from the denominator of the second term. Despite the complexity of the biological reaction, pseudo-first-order rate constants are useful to

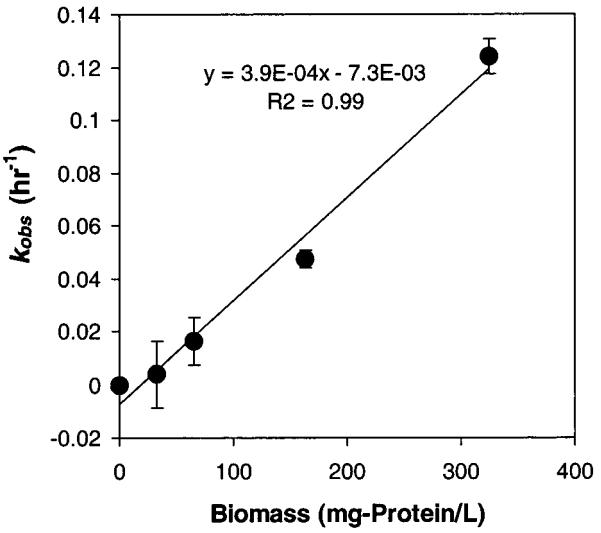

FIGURE 3. Pseudo-first-order rate constants for CT transformation at various biomass concentrations of *G. metallireducens* (average $CT_0 = 4.0 \pm 0.3$ μM). Data points report the average of duplicate vials. Error bars represent one standard deviation.

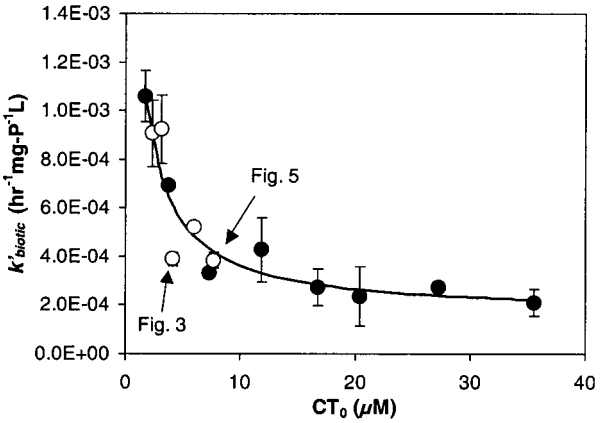

FIGURE 4. Protein-normalized pseudo-first-order rate constants for CT transformation by *G. metallireducens* as a function of initial CT concentration (CT_0 = 1.7−35.6 μM) (●). Data points report the average of duplicate vials. Error bars represent one standard deviation. For comparison, protein-normalized rates from five additional experiments are also included (○). Solid line shows the least-squares best fit of eq 3.

enable direct comparisons with the abiotic rate studies. Protein-normalized pseudo-first-order rate constants can be estimated by rearrangement of eq 2 as follows:

$$k'_{\text{biotic}} = \frac{k_{\text{biotic}}}{X_0} \approx \frac{-(\mathrm{d}C/\mathrm{d}t)_0}{C_0 X_0} = \left(\frac{\nu_1^{\max}}{K_1 + C_0}\right) + \left(\frac{\nu_2^{\max}}{K_2}\right) \quad (3)$$

where k'_{biotic} is the protein-normalized pseudo-first-order rate constant (h^{-1} (mg of protein)$^{-1}$ L). Values for the kinetic parameters $\nu_1^{\max} = 2.07 \times 10^{-3} \pm 9.0 \times 10^{-4}$ (μM h^{-1} (mg of protein)$^{-1}$ L), $K_1 = 0.51 \pm 0.96$ (μM), and $\nu_2^{\max}/K_2 = 1.64 \times 10^{-4} \pm 7.7 \times 10^{-5}$ (h^{-1} (mg of protein)$^{-1}$ L) were estimated by nonlinear least-squares fitting of eq 3 to the observed pseudo-first-order rate constants at all starting CT concentrations. For comparison, the fitted model is included in Figure 4.

Most published models of CT co-metabolism assume either a first-order dependence on CT concentration (*9*, *26*, *45*−*47*) or employ a modification of a one-site Michaelis−Menten or Monod expression (*48*, *49*). Although the proposed two-site Michaelis−Menten model is novel in this application, no mechanistic interpretation should be inferred since no independent evidence of multiple reaction sites was obtained. Furthermore, as the reaction is not truly first-order (Figure 4), eq 3 and the fitted rate parameters must be considered empirical. Nevertheless, the model generates pseudo-first-order rate constants that are in close agreement with the experimentally observed values and is therefore useful for the purposes of this study.

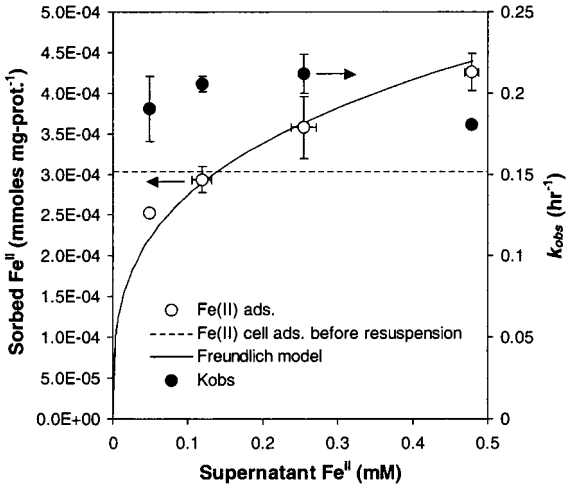

FIGURE 5. Comparison of pseudo-first-order rate constants for CT transformation by *G. metallireducens* cells at varying loadings of Fe^{II} (biomass = 514 ± 19 mg L^{-1}, average $CT_0 = 7.7 \pm 0.7$ μM). Data points report the average of duplicate vials. Error bars represent one standard deviation. Solid line shows the least-squares best-fit Freundlich model, $[Fe^{II}]_{ads} = k_f[Fe^{II}]_{aq}^n$, where $k_f = 5.48 \times 10^{-4}$ and $n = 3.00 \times 10^{-1}$. Units of $[Fe^{II}]_{ads}$ and $[Fe^{II}]_{aq}$ are in mmole (mg of protein)$^{-1}$ and in mM, respectively. See text for discussion of isotherm.

Effect of Fe^{II} Cell Sorption on CT Transformation Rates. To investigate the impact of cell-associated Fe^{II} on CT transformation kinetics, an Fe^{II} sorption isotherm and CT transformation rate study was conducted in resting cell suspensions of *G. metallireducens*. Ferrous iron can adsorb to cells by forming ligand complexes with a variety of surface functional groups including amino, carboxyl, hydroxyl, and phosphate groups (*50*). Fe^{II}−surface complexes can be stronger reductants than Fe^{2+}(aq) (*20*) and could potentially enhance CT transformation. Alternatively, adsorbed Fe^{II} may block reactive sites on the cell surface and inhibit reaction. Ferrous iron adsorption on cells has been shown to inhibit Fe^{III} reduction in *Shewanella* strains (*51*, *52*).

The cells used in the Fe^{II} sorption study were grown on Fe^{III}−citrate media and retained some residual Fe^{II} at the beginning of the experiment (~3.05×10^{-4} mmol of Fe^{II}/mg of protein, see Figure 5). As a result of this preassociated iron, the lowest supernatant concentrations on the isotherm increased to 0.05 and 0.12 mM Fe^{II}(aq) due to Fe^{II} desorption from the cells, while the highest two concentrations decreased due to cell sorption. Assuming that hysteresis was not significant (*53*), the data are well-described by a Freundlich isotherm (Figure 5). CT transformation was monitored in each suspension over approximately 2 half-lives. The resulting pseudo-first-order rate constants are also shown in Figure 5. The plot shows no significant change in CT transformation rates regardless of the amount of Fe^{II} associated with the cells. This suggests that ferrous iron sorbed to cells is not a significant source of CT reactivity. Furthermore, CT depletion rates were not diminished by ferrous iron sorption, indicating that Fe^{II} does not block the sites responsible for CT transformation in *G. metallireducens*.

Characterization of Biogenic Magnetite. Transmission electron microscopy of the biogenic magnetite collected at

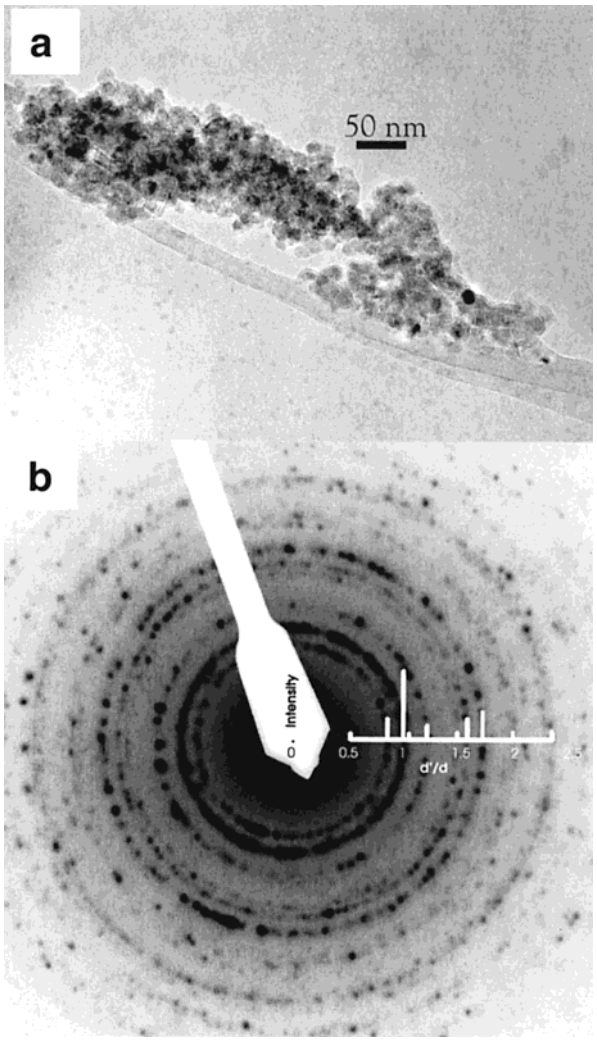

FIGURE 6. (a) Transmission electron micrograph of biogenic magnetite particles. Particle diameters vary between 5 and 30 nm (mean diameter = 15.5 ± 4.6 nm). (b) Selected area electron diffraction (SAED) for the same biogenic magnetite particle agglomerate. The proportional spacing and expected relative intensities of the 10 most prominent diffraction lines for magnetite (Fe_3O_4) are superimposed for comparison.

565 days revealed that the solids consisted predominantly of ultra fine particles 5−30 nm in diameter (Figure 6a). Selected area electron diffraction (SAED) of the particles revealed rings and spots consistent with randomly oriented magnetite crystals (Figure 6b). No extraneous diffraction lines were observed, indicating that, within the microprobe analysis area (≈0.2 μm^2), no other crystal structures were evident. Unlike SAED, X-ray diffraction provides bulk sample information. The XRD results (Figure 7a) show peaks indicative of magnetite and a second mineral, siderite ($FeCO_3$). Siderite formation has often been reported in carbonate-buffered iron-reducing cultures (*54*−*57*).

The ferrous iron content of the biogenic magnetite (35.1 ± 1.8%) slightly exceeded that expected in stoichiometric magnetite (33.3% Fe^{II}/Fe^{TOT}). This difference can be attributed to the siderite fraction. Assuming that siderite and magnetite are the only minerals present and considering the average error associated with the ferrous extraction analysis (±1.8%), siderite content could vary from a negligible amount to as much as 2.8% by mass. Although small, the siderite fraction had an important effect on Fe^{II} solubility in the biogenic magnetite suspensions. Because the resuspension buffer contained no carbonate, the resulting slurries were under-

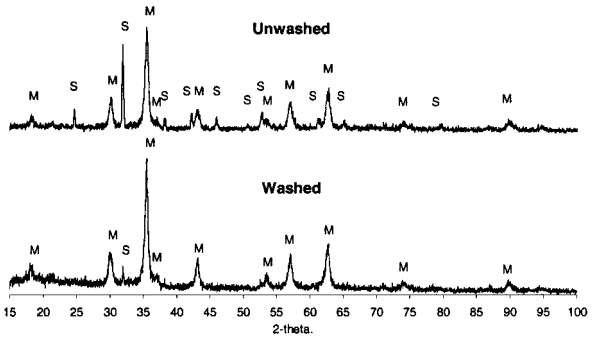

FIGURE 7. X-ray diffraction spectra of biogenic magnetite before (a) and after (b) long-term washing in anoxic buffer (10 mM MOPSO, pH 7.0). M = magnetite (Fe_3O_4), S = siderite ($FeCO_3$).

TABLE 1. Potential Contributions of Siderite and Magnetite to Total Surface Area

compd	particle diameter (nm)	density (g/cm^3)	specific surf. area[a] (m^2/g)	mass fraction (%)	surf. fraction (%)
$FeCO_3$	1000	3.8	1.58	2.8[b]	0.1
Fe_3O_4	16	5.18	72.4	97.2	99.9

[a] Based on spherical particles: SSA = 3/(density × radius). [b] Assumes siderite present at the highest mass percent within the standard error of the Fe^{II}/Fe^{TOT} extraction measurement.

saturated with respect to the solubility product of $FeCO_3$. As a result, transfer of the biogenic $Fe_3O_4/FeCO_3$ mixture to MOPSO buffer consistently resulted in a gradual accumulation of Fe^{II}(aq) from siderite dissolution. Evidence to support this mechanism is shown in Figure 7b, where the XRD of the biogenic minerals showed near-complete disappearance of the siderite diffraction peaks after prolonged washing with the resuspension buffer (10 mM MOPSO, pH 7.0), while magnetite peaks were preserved.

The BET specific surface areas of biogenic magnetite aged 124 or 565 days were similar, 77.5 ± 0.3 and 68.9 ± 0.3 m^2 g^{-1}, respectively. It is instructive to look at the potential contributions of siderite and magnetite to the total surface area of the solids. Siderite particles produced in iron-reducing cultures have previously been described as relatively large in diameter (1−25 μm) (*55*, *57*). Using a conservative diameter for siderite of 1 μm and a diameter of 16 nm for the biogenic magnetite, an average based on particle measurements from Figure 6a, the percent contributions of each mineral to total surface area were estimated on the basis of spherical particles (Table 1). Assuming siderite is present at the estimated upper limit of 2.8% by mass, magnetite still accounts for 99.9% of the total surface area. This indicates that, even though siderite controls Fe^{II} solubility, magnetite remains the predominant mineral at the solid/solution interface.

Abiotic Transformation of CT by Biogenic Fe_3O_4. The abiotic transformation of CT followed first-order kinetics under all test conditions. No reaction was observed in buffer controls or filtered buffer preequilibrated with the biogenic solids, indicating that the reaction is surface-mediated. Plotting the headspace adjusted pseudo-first-order rate constants against the surface area loading for both magnetites, the data collapse to a single linear relationship shown in Figure 8. The linearity demonstrates that the pseudo-first-order rate constants are proportional to magnetite surface area concentration, allowing prediction of the abiotic rate from the following simple expression:

$$k_{abiotic} = k'_{abiotic} M_0 \quad (4)$$

where $k_{abiotic}$ is the pseudo-first-order rate constant for the

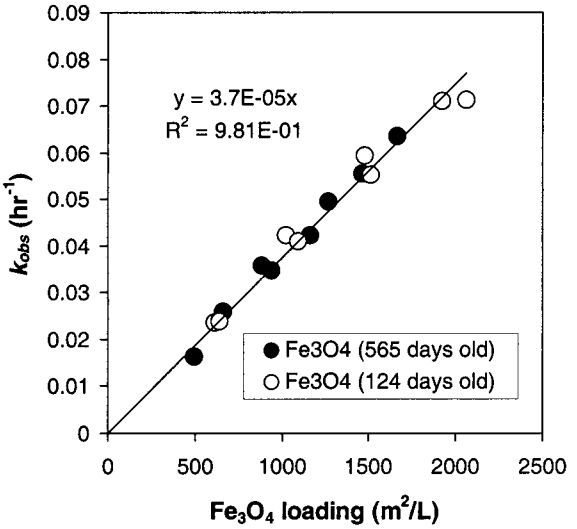

FIGURE 8. Dependence of abiotic pseudo-first-order rate constant on surface area concentration ($m^2\ L^{-1}$) of biogenic magnetite aged 124 (○) or 565 (●) days (pH 7.0, average $CT_0 = 18.7 \pm 1.4\ \mu M$, $I = 0.1$ M $NaClO_4$). Aqueous Fe^{II} concentrations measured in the suspensions at the beginning of the CT rate experiments were 570 μM and 670 μM for the 124- and 565-day-old magnetite particles, respectively (see text for discussion).

mineral-mediated reaction (h^{-1}), $k'_{abiotic}$ is the surface area concentration normalized rate constant $= 3.70 \times 10^{-5} \pm 5 \times 10^{-7}$ ($h^{-1}\ m^{-2}\ L$) (from Figure 8), and M_0 is the surface area concentration of biogenic magnetite ($m^2\ L^{-1}$). The linearity also indicates that no significant differences existed in the surface reactivity of the 565- and 124-day-old magnetites.

Interpretation of the abiotic kinetics requires further consideration of the solution chemistry in this system. As discussed earlier, siderite controls Fe^{II}(aq) concentrations in the biogenic magnetite suspensions through dissolution/precipitation reactions. By extension, siderite must also control the activity of surface-adsorbed Fe^{II} through an appropriate equilibrium relationship. Prior to conducting the abiotic kinetic studies, the solids were equilibrated in the fresh buffer for a period of 7 days, at which point the Fe^{II}(aq) concentrations in suspensions of the 124- and 565-day-old magnetites had risen to 570 and 670 μM, respectively. To the authors' knowledge, the only published isotherm for Fe^{II} adsorption on magnetite at pH 7.0 is the work of Klausen et al. (*38*), who found that equilibrium Fe^{II}(aq) concentrations over 500 μM correspond to near-saturation of the magnetite surface. This implies that siderite, through control of Fe^{II}(aq) concentrations, maintains the magnetite surfaces at near-saturation coverage of adsorbed Fe^{II}. Pecher et al. (*58*) presented evidence that surface precipitation was likely an important phenomenon at circumneutral pH when Fe^{II} adsorption on magnetite exceeded 60% of saturation. The surface area-normalized kinetics for CT transformation by biogenic magnetite (Figure 8), therefore, likely represent magnetite reactivity at high Fe^{II}(ads) loadings and may involve surface precipitates.

Biotic and Abiotic Contributions to CT Transformation in Whole Cultures. The relative contributions of biotic and abiotic reactions to CT transformation were assessed when cells and minerals were present together. Total protein (X_0) and mineral surface area (M_0) were measured at several time points in an active iron-reducing culture (Figure 9a) and substituted into the biomass- and surface area-normalized rate expressions (eqs 3 and 4) to derive pseudo-first-order rate constants for each reaction (k_{biotic} and $k_{abiotic}$) (Figure 9b). Growth commenced shortly after inoculation of the IR media with *G. metallireducens*, reaching a maximum protein

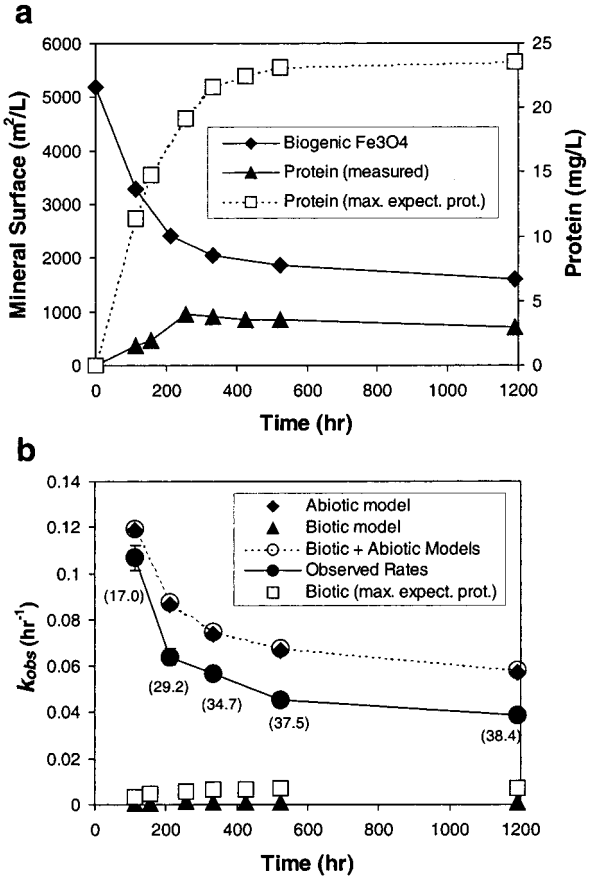

FIGURE 9. (a) Time course changes in total protein and mineral surface area concentration during microbial reduction of HFO by *G. metallireducens*. See text for discussion of maximum expected protein yield. (b) Comparison of predicted biotic and abiotic rates of CT transformation to actual rates observed in the model system during microbial reduction of HFO by *G. metallireducens* (average $CT_0 = 14.2 \pm 0.7\ \mu M$). Parentheses show the measured fractional percent of Fe^{II}/Fe^{TOT} in the biogenic solids at each sample point.

concentration of 4.0 mg L^{-1} at 257 h of incubation. The cessation of protein accumulation corresponded well with a marked decrease in acetate consumption and iron reduction, consistent with the onset of growth-limiting conditions (data not shown). The initial SSA for the freeze-dried HFO was $302 \pm 1.9\ m^2\ g^{-1}$, in close agreement with other studies of this material (*59*, *60*). After inoculation, the specific surface areas decreased rapidly and then slowed as microbial iron reduction became limited. At the end of the incubation period (1190 h), the SSA was found to be $134 \pm 0.3\ m^2\ g^{-1}$. The final proportion of Fe^{II}/Fe^{TOT} in the biogenic magnetite was found to be $38.8 \pm 1.8\%$ or approximately 60−65 mM Fe^{II} on a total concentration basis.

The growth of *G. metallireducens* on HFO and acetate was first described by Lovley and Phillips (*40*), who reported a maximum cell density of approximately 2.8×10^8 cells mL^{-1} using nearly identical media. Combining the same protein extraction/assay used in the kinetic experiments with direct counts of *G. metallireducens* bacteria (Fe^{III}−citrate grown), the average extracted protein was estimated to be $4.5 \times 10^{-11} \pm 1.4 \times 10^{-11}$ mg $cell^{-1}$ ($n = 3$). Using this value, the cell yield of 4.0 mg L^{-1} translates to a maximum cell count of 8.9×10^7 cells mL^{-1}, or approximately 32% of the yield reported by Lovley and Phillips (*40*). The low yield may simply indicate that total protein was underestimated due to extraction inefficiencies or interference brought about by the presence of the iron oxide solids. Alternatively, the protein content

per cell may actually be lower when grown on HFO rather than Fe^{III}−citrate (*61*). Normalized by the quantity of iron reduced, cell yields for DIRB grown on a variety of substrates and iron oxides are remarkably similar ranging from 2.0 to 6.4×10^9 cells $mmol^{-1}$ Fe^{II} (*40*, *52*, *62*−*66*). By assuming the highest cell yield for any DIRB (6.4×10^9 cells $mmol^{-1}$ Fe^{II}) and applying a protein content of 5.9×10^{-11} mg $cell^{-1}$ (highest value within the standard error for the measurement for Fe^{III}−citrate-grown cells), a reasonably conservative estimate of maximum expected protein yield can be calculated on the basis of total Fe^{II} formed in the IR media. For comparison, these values are also presented in Figure 9a. Regardless of any potential inefficiency in the protein extraction, the same method was applied consistently throughout the work, therefore, providing a basis for relative biomass comparisons.

Defining the overall model as the sum of the biotic and abiotic pseudo-first-order rate constants ($k_{model} = k_{biotic} + k_{abiotic}$), Figure 9b reveals the actual measured rates of CT transformation in whole culture to be approximately 12−35% lower than predicted. Although the cause of the discrepancy cannot be determined from these data, we speculate that buffer effects (HCO_3^- vs MOPSO) or sorption of cells and organic matter to reactive surface sites may be responsible. Despite the model overestimation, the results show that the dechlorination rates in the whole culture can almost entirely be ascribed to abiotic surface-mediated reactions, the biotic contribution (based on actual protein measurements) being approximately 2 orders of magnitude (40−230-fold) smaller than the observed whole culture rates, and 60−260-fold smaller than the abiotic model rates (Figure 9b). Estimating the biotic contribution on the basis of the maximum expected protein yield (approximately 6 times larger than the measured yield) still predicts a strong predominance of abiotic reactivity. The close parallel trends in k_{obs} and mineral surface area concentration also support the conclusion that mineral surfaces rather than biomass govern the transformation rates. The proportionality of the reaction rates to mineral surface area even at the earliest stages of iron reduction, when the stoichiometry of Fe^{II}/Fe^{TOT} (17%) was well below that of magnetite (33%), suggests that Fe_3O_4 formation is not required for the reaction to proceed and that surface-adsorbed Fe^{II} may be the principal reductant.

Environmental Significance. The relative contributions of biotic and abiotic reactions to contaminant transformation in soils have long been debated (*67*, *68*). The hypothesis that microbial reduction of iron can indirectly drive abiotic transformation of contaminants was first proposed by Glass (*21*) to explain the reductive dechlorination of DDT in flooded soils. Since then, a growing body of literature has demonstrated the importance of biologically generated surface Fe^{II} to contaminant fate in iron-reducing environments. Using Arrhenius studies and nitroaromatic probe compounds (NAC) in a similar model iron-reducing system to this study, Heijman et al. (*36*, *37*) and Klausen et al. (*38*) demonstrated that the reduction of the NACs was predominantly an abiotic process mediated by biogenic Fe^{II} adsorbed to magnetite surfaces. Several researchers have recently shown that reduced iron oxides or hydroxides generated by DIRB can transform CT in subsequent abiotic reactions (*27*−*30*). The results from this study demonstrate that a second member of the dissimilative iron-reducing bacteria, *G. metallireducens*, can biotically transform CT. Yet, in the presence of HFO, *G. metallireducens* drives CT transformation primarily through the formation of reactive mineral surfaces. Although this suggests that biologically activated mineral surfaces may be the principal agents of reductive transformation in iron-reducing environments, it does not diminish the role that DIRB play. Without *G. metallireducens*, no iron reduction and, therefore, no CT reduction would have occurred in this model system.

Although caution is needed in extrapolating laboratory results to field conditions, these findings suggest that an alternative approach to stimulate reductive transformation of contaminants in iron-reducing environments may be to enhance the formation of reactive biogenic minerals in situ. While magnetite is not commonly encountered in typical surface sediments (*16*), other Fe^{II} species have been identified in iron-reducing environments that are also reactive with chlorinated solvents including ferrous sulfides (*33*, *43*), green rusts (*31*, *32*), and sorbed (or surface precipitated) Fe^{II} (*27*−*30*). Field evidence already exists linking surface associated biogenic Fe^{II} with CT transformation in contaminated aquifer plumes (*69*−*71*). It might also be possible to couple microbial iron reduction to reactive barrier design to exploit the ability of these bacteria to reactivate passivated metal surfaces (*72*). Further investigation of the effect that cell/mineral interactions have on contaminant fate should yield a better understanding of natural attenuation in iron-reducing environments and could lead to the development of novel bioremediation strategies.

Acknowledgments

The authors thank Derek Lovely and Jocelyn Fraga, University of Massachusetts, Amherst, for kindly providing the *G. metallireducens* culture used in this work; Corrina Wauchope, Electron Micro-beam Analysis Laboratory (EMAL), University of Michigan, for assistance in the transmission electron microscopy work; Michael Keinath for BET analyses; and Tom Yavaraski for various technical assistance. Michael Gerdenich, Cyndee Gruden, Kim Hayes, and Jeremy Semrau provided helpful comments during manuscript preparation. M.L.M. completed a portion of this work while visiting the Department of Geography and Environmental Engineering, Johns Hopkins University (1997−1998). This work was supported by EPA Grant R-819605-01-4 and EPA STAR Fellowship U-915327-01-0.

Literature Cited

(1) Westrick, J. J.; Mello, J. W.; Thomas, R. F. *J. Am. Water Works Assoc.* **1984**, *76* (5), 52−59.
(2) Bouwer, E. J.; McCarty, P. L. *Appl. Environ. Microbiol.* **1983**, *45*, 1286−1294.
(3) Mohn, W.; Tiedje, J. M. *Microbiol. Rev.* **1992**, *56* (3), 482−507.
(4) Kriegman-King, M. R.; Reinhard, M. *Environ. Sci. Technol.* **1992**, *26*, 2198−2206.
(5) Kriegman-King, M. R.; Reinhard, M. *Environ. Sci. Technol.* **1994**, *28*, 692−700.
(6) Curtis, G. P. Ph.D. Dissertation, Stanford University, 1991.
(7) Criddle, C. S.; McCarty, P. L. *Environ. Sci. Technol.* **1991**, *25*, 973−978.
(8) Egli, C.; Stromeyer, S.; Cook, A. M.; Leisinger, T. *FEMS Microbiol. Lett.* **1990**, *68*, 207−212.
(9) Criddle, C. S.; DeWitt, J. T.; Grbic-Galic, D.; McCarty, P. L. *Appl. Environ. Microbiol.* **1990**, *56*, 3240−3246.
(10) Holliger, C.; Schraa, G. *FEMS Microbiol. Rev.* **1994**, *15*, 297−305.
(11) Holliger, G. C.; Stams, A. J. M.; Zehnder, A. *Appl. Environ. Microbiol.* **1993**, *59*, 2991−2997.
(12) Krumholz, L. R.; Sharp, R.; Fishbain, S. S. *Appl. Environ. Microbiol.* **1996**, *62*, 4108−4113.
(13) Maymo-Gatell, X.; Chien, Y. T.; Gossett, J. M.; Zinder, S. H. *Science* **1997**, *276*, 1568−1571.
(14) Coey, J. M. D.; Schindler, D. W.; Weber, F. *Can. J. Earth Sci.* **1974**, *11*, 1489−1493.
(15) Nealson, K. H.; Myers C. R. *Appl. Environ. Microbiol.* **1992**, *58*, 439−443.
(16) Thamdrup, B. *Adv. Microb. Ecol.* **2000**, *16*, 41−84.
(17) Lovley, D. R. In *The Prokaryotes*; Dworkin, M., Falkow, S., Rosenberg, E., Schleifer, K. H., Stackebrandt, E. Eds.; Springer-Verlag: New York, 2000. http://www.prokaryotes.com (accessed Aug 2001).

(18) Madigan, M. T.; Martinko, J. M.; Parker, J. *Brock Biology of Microorganisms*, 9th ed.; Prentice Hall: Upper Saddle River, NJ, 2000; p A-4.
(19) Totten, L. A.; Roberts, A. L. *Crit. Rev. Environ. Sci. Technol.* **2001**, *31* (2), 175−221.
(20) Stumm, W.; Sulzberger, B. *Geochim. Cosmochim. Acta.* **1992**, *56*, 3233−3257.
(21) Glass, B. L. *J. Agric. Food Chem.* **1972**, *20*, 324−327.
(22) MaCalady, D. L.; Tratnyek, P. G.; Grundl, T. J. *J. Contam. Hydrol.* **1986**, *1*, 1−28.
(23) Vogel, T. M.; Criddle, C. S.; McCarty, P. L. *Environ. Sci. Technol.* **1987**, *21*, 722−736.
(24) Picardal, F. W.; Arnold, R. G.; Couch, H.; Little, A. M.; Smith, M. E. *Appl. Environ. Microbiol.* **1993**, *59*, 3763−3770.
(25) Picardal, F. W.; Arnold, R. G.; Huey, B. B. *Appl. Environ. Microbiol.* **1995**, *61*, 8−12.
(26) Petrovskis, E. A.; Vogel, T. M.; Adriaens, P. *FEMS Microbiol. Lett.* **1994**, *121*, 357−364.
(27) Fredrickson, J. K.; Gorby, Y. A. *Curr. Opin. Biotechnol.* **1996**, *7*, 287−294.
(28) Amonette, J. E.; Workman, D. J.; Kennedy, D. W.; Fruchter, J. S.; Gorby, Y. A. *Environ. Sci. Technol.* **2000**, *34*, 4606−4613.
(29) Kim, S.; Picardal, F. W. *Environ. Toxicol. Chem.* **1999**, *18*, 2142−2150.
(30) Picardal, F. W.; Kim, S.; Radue, A.; Backhus, D. In *Emerging Technologies in Hazardous Waste Management 7*; Tedder, D. W., Pohland, F. G., Eds.; Plenum Press: New York, 1997; pp 81−90.
(31) Erbs, M.; Hansen, J. C. B.; Olsen C. E. *Environ. Sci. Technol.* **1999**, *33*, 307−311.
(32) O'Laughlin, E. J.; Burris, D. R. *Preprints of Papers Presented at the 219th ACS National Meeting*, San Francisco, CA; American Chemical Society: Washington, DC, 2000; Vol. 40 (1), pp 62−63.
(33) Butler, E. C.; Hayes, K. F. *Environ. Sci. Technol.* **2000**, *34*, 422−429.
(34) McCormick, M. L.; Kim, H. S.; Bouwer, E. J.; Adriaens, P. *Proceedings of the 30th Mid-Atlantic Industrial and Hazardous Waste Conference*; Technomic Publishing: Lancaster, PA, 1998; pp 339−349.
(35) McCormick, M. L.; Adriaens, P. *Preprints of Papers Presented at the 220th ACS National Meeting*, Washington, DC; American Chemical Society: Washington, DC, 2000; Vol. 40 (2), pp 357−361.
(36) Heijman, C. G.; Holliger, C.; Glaus, M. A.; Schwarzenbach, R. P.; Zeyer, J. *Appl. Environ. Microbiol.* **1993**, *59*, 4350−4353.
(37) Heijman, C. G.; Grieder, E.; Holliger, C.; Schwarzenbach, R. P. *Environ. Sci. Technol.* **1995**, *29*, 775−783.
(38) Klausen, J.; Trober, S. P.; Haderlein, S. B.; Schwarzenbach, R. P. *Environ. Sci. Technol.* **1995**, *29*, 2396−2404.
(39) Peterson, M. L.; White A. F.; Brown, G. E., Jr.; Parks, G. A. *Environ. Sci. Technol.* **1997**, *31*, 1573−1576.
(40) Lovley, D. R.; Phillips, E. J. P. *Appl. Environ. Microbiol.* **1988**, *54*, 1472−1480.
(41) Lovley, D. R.; Giovannoni, S. J.; White, D. C.; Champine, J. E.; Phillips, E. J. P.; Gorby, Y. A.; Goodwin, S. *Arch. Microbiol.* **1993**, *159*, 336−344.
(42) Stookey, L. L. *Anal. Chem.* **1970**, *42* (7), 779−781.
(43) Butler, E. C.; Hayes, K. F. *Environ. Sci. Technol.* **1999**, *33*, 2021−2027.
(44) Gossett, J. M. *Environ. Sci. Technol.* **1987**, *21*, 202−208.
(45) Hooker, B. S.; Skeen, R. S.; Petersen, J. N. *Biotechnol. Bioeng.* **1994**, *44*, 211−218.
(46) Doong, R. A.; Chen, T. F.; Wu, Y. W. *Appl. Microbiol. Biotechnol.* **1997**, *47*, 317−323.
(47) Zou, S.; Stensel, H. D.; Ferguson, J. F. *Environ. Sci. Technol.* **2000**, *34*, 1751−1757.
(48) Doong, R. A.; Wu, S. C. *Water Res.* **1996**, *30* (3), 577−586.
(49) Ely, R. L.; Williamson, K. J.; Hyman, M. R.; Arp, D. J. *Biotechnol. Bioeng.* **1997**, *54*, 520−534.
(50) Beveridge, T. J.; Murray, R. G. E. *J. Bacteriol.* **1980**, *141* (2), 876−887.
(51) Urrutia, M. M.; Roden, E. E.; Fredrickson, J. K.; Zachara, J. M. *Geomicrobiology* **1998**, *15*, 269−291.
(52) Liu, C.; Zachara, J. M.; Gorby, Y. A.; Szecsody, J. E.; Brown, C. F. *Environ. Sci. Technol.* **2001**, *35*, 1385−1393.
(53) Fowle, D. A.; Fein, J. B. *Chem. Geol.* **2000**, *168*, 27−36.
(54) Sparks, N. H. C.; Mann, S.; Bazylinski, D. A.; Lovley, D. R.; Jannasch, H. W.; Frankel, R. B. *Earth Planet. Sci. Lett.* **1990**, *98* (1), 14−22.
(55) Mortimer, R. J. G.; Coleman, M. L. *Geochim. Cosmochim. Acta* **1997**, *61*, 1705−1711.
(56) Zhang, C.; Liu, S.; Phelps, T. J.; Cole, D. R.; Horita, J.; Fortier, S. M.; Elless, M.; Valley, J. W. *Geochim. Cosmochim. Acta* **1997**, *61*, 4621−4632.
(57) Fredrickson, J. K.; Zachara, J. M.; Kennedy, D. W.; Dong, H.; Onstott, T. C.; Hinman, N. W.; Li, S. *Geochim. Cosmochim. Acta* **1998**, *62*, 3239−3257.
(58) Pecher, K.; Haderlein, S. B.; Schwarzenbach, R. P. *Preprints of Papers Presented at the 213th ACS National Meeting*, San Francisco, CA; American Chemical Society: Washington, DC, 1997; Vol. 37 (1), pp 185−187.
(59) Van der Woude, J. H. A.; De Bruyn, P. L. *Colloid Surf.* **1983**, *8*, 55−78.
(60) Lewis, D. G.; Schwertmann, U. *J. Colloid Interface Sci.* **1980**, *78*, 543−553.
(61) Bond, D. R. University of Massachusetts, Amherst, personal communication, 2001.
(62) Lovley, D. R.; Lonergan, D. J. *Appl. Environ. Microbiol.* **1990**, *56*, 1858−1864.
(63) Johnson, D. B.; McGinness, S. *Appl. Environ. Microbiol.* **1991**, *57*, 207−211.
(64) Caccavo, F.; Blakemore, R. P.; Lovley, D. R. *Appl. Environ. Microbiol.* **1992**, *58*, 3211−3216.
(65) Caccavo, F.; Lonergan, D. J.; Lovley, D. R.; Davis, M.; Stolz, J. F.; McInerney, J. *Appl. Environ. Microbiol.* **1994**, *60*, 3752−3759.
(66) Roden, E. E.; Zachara, J. M. *Environ. Sci. Technol.* **1996**, *30*, 1618−1628.
(67) Temme, J. *Plant Soil* **1948**, *1*, 145−166.
(68) Alexander, M. In *Agriculture and the Quality of our Environment*; Brady, N. C., Ed.; American Association for the Advancement of Science 85; AAAS: Washington, DC, 1967; pp 331−342.
(69) Nielsen, P. H.; Bjarnadottir, H.; Winger, P. L.; Christensen, T. H. *J. Contam. Hydrol.* **1995**, *20*, 51−66.
(70) Rugge, K.; Hofstetter, T. B.; Haderlein, S. B.; Bjerg, P. L.; Knudsen, S.; Zraunig, C.; Mosbæk, H.; Christensen, T. H. *Environ. Sci. Technol.* **1998**, *32*, 23−31.
(71) Bjerg, P. L.; Rugge, K.; Cortsen, J.; Nielson, P. H.; Christensen, T. H. *Ground Water* **1999**, *37*, 113−121.
(72) Gerlach, R.; Cunningham, A. B.; Caccavo, F. *Environ. Sci. Technol.* **2000**, *34*, 2461−2464.

Received for review May 2, 2001. Revised manuscript received September 17, 2001. Accepted October 3, 2001.

ES010923+